

Received January 11, 2017; accepted February 3, 2017, date of publication February 14, 2017, date of current version March 13, 2017.

Digital Object Identifier 10.1109/ACCESS.2017.2668523

Adaptive Solitary Pulmonary Nodule Segmentation for Digital Radiography Images Based on Random Walks and Sequential Filter

DAN WANG¹, JUNFENG WANG¹, YIHUA DU², AND PENG TANG³

¹College of Computer Science, Sichuan University, 610065 Chengdu, China

²Affiliated Hospital of Southwest Medical University, 646000 Luzhou, China

³School of Electrical Engineering, Southwest Jiaotong University, 610031 Chengdu, China

Corresponding author: J. Wang (wangjf@scu.edu.cn)

This work was supported in part by the National Science and Technology Major Project under Grant 2012ZX10004-901, in part by the Provincial Key Science and Technology Research and Development Program of Sichuan, China under Grant 2013SZ0002, Grant 2014SZ0109, and Grant 2016ZR0087, and in part by the the Ph.D. Program Foundation of Ministry of Education of China under Grant 20130181110095.

ABSTRACT Solitary pulmonary nodules (SPN) in digital radiography (DR) images often have unclear contours and infiltration, which make it a challenging task for traditional segmentation models to get satisfactory segmentation results. To overcome this challenge, this paper has proposed an adaptive SPN segmentation model for DR images based on random walks segmentation and sequential filter. First, the SPN image is decomposed to get the cartoon component, which is used to acquire a set of seeds. Second, the seeds selection tactic is employed to optimize the scope of walking pixels and reduce the number of seeds, which could reduce the computational cost. Finally, we incorporate the sequential filter and construct the new representation of the weight and the probability matrices. In this paper, by using a data set of 724 SPN cases, the proposed method was tested and compared with four different models, and five kinds of evaluation indicators were given to evaluate the effect of segmentation. Experimental results indicate that the proposed method performs well on the blurred edge, as it could get relatively accurate results.

INDEX TERMS Image segmentation, random walks, sequential filter, digital radiography, solitary pulmonary nodule.

I. INTRODUCTION

Lung cancer ranks first in the death of malignant tumor as reported by the World Health Organization [1]. Therefore, early detection and treatment are important to reduce the mortality of lung cancer. Solitary Pulmonary Nodule (SPN) is one of the important characteristic of early lung cancer. The location, the size and the rate of the growth are important indicators for diagnosis [2]. The accuracy of SPN segmentation is essential to judge the real condition. The correct segmentation results are the premise of feature extraction and character analysis [3]. Due to unique noise characteristics in medical images we do not have common techniques suitable for all segmentation problems.

Digital Radiography [4], Computerized Tomography [5], Magnetic Resonance Imaging [6] (abbreviated as DR, CT, MRI, respectively) are medical imaging techniques used in lung imaging in recent years. Researchers have done a lot of work on CT pulmonary nodules segmentation, and several lung CT image databases were built. But there are still seldom

researches on DR images. The DR technology performs better than CT and MRI in terms of the equipment cost and the skill requirements of operating personnel [7]. It is widely used in economical and medical backward areas [8]. Therefore, it is of great practical significance to reduce the mortality of lung cancer in remote area.

Unlike CT images, DR images lack of tomography information [9]. It is represented as just one image. In general, the center of the SPN is characterized as high brightness, and tissues near the margin of the lesion often show as fuzzy thin shadow. In most images, the edges of SPN are blurred even missing [10]. The fuzzy clustering [11] method is widely employed in medical image processing. Too many improvements have been made to adapt to lesion segmentation. The lung parenchyma is divided into several clusters, and different processing methods were constructed to get the region of interest. Claus' [12] clustering algorithm can handle the vessel, crossing point and the solitary nodule. But it mainly focuses on detecting nodules for

CAD systems, and does not care other features. Besides, the complex clustering brings much time consumption. Genetic Algorithm Template Match [13] (GATM) was also employed, different size of Gauss templates were selected to implement fast template matching. Ozekes [14] did the further study, where the improved algorithm can automatically process the image, which is suitable for CAD system, yet the results are still unsatisfactory. Besides, the geometric active contour models perform well on topological deformation [15], such as merge and split, so it was widely introduced to deal with the medical images. Chan and Vese [16] algorithm can segment the objects by the regional information, which doesn't rely on boundaries defined by gradients. Nevertheless, the difference of nodules' surrounding region is quite small, and surrounding tissue has a smooth gray change. There is often over-segmentation when segmenting the DR nodules.

Overall, the classical algorithms, such as clustering, template match and region-based active contour algorithm, cannot handle the structure characteristics of nodules. Grady [17] proposed the random walks image segmentation method, which is an interactive image segmentation method based on graph theory. Image to be segmented is transformed into a weighted undirected graph. The segmentation result is affected by the definition of weight, and finally determined by the pre-labeled pixels (referred to as seeds). The method is insensitive to noise and could suppress the influence of the boundary deletion [18]. However, it is obvious that manually labeling the seed point is the short board and easily affected by uncontrollable conditions. Hao [19] proposed an automatic method which was specially designed for mammograms. The differences of histopathologic structures decide that it is not suitable for DR pulmonary nodules segmentation, and the method incorporates CV algorithm which is time-consuming.

In this paper, we analyze the structure of the DR pulmonary nodules, and present an improved adaptive random walks segmentation which integrates sequential filter. Firstly, the original SPN image is decomposed into texture and cartoon components which is used to get the seeds. Secondly, based on the seeds, the walker pixels and seeds selection tactic are employed to reduce the computational overhead. Then, we incorporate the sequential filter to random walks, and define the improved weight representation and probability matrices. Finally, the proposed method is exploited to get the segmentation results. The proposed method has the properties as below:

1. The fast seeds acquisition method that is based on the cartoon component could fast and effectively get the seeds without iteration.
2. Seeds selection tactic optimally selects the walking pixels and reduce the number of seeds. This tactic could avoid contour leaking and reduce computational cost at the same time.
3. Its combination with the sequential filter could smooth the inhomogenous region and avoid over-smoothing.

The newly defined weight representation and probability matrices could improve the segmentation.

4. The proposed method could ensure the precise segmentation results even the image definition is poor.

II. PREVIOUS WORK

A. THE SEQUENTIAL FILTER

The Gaussian smoothing is the isotropic point diffusion. The smoothing ability of the Gaussian function relies on the parameter σ [20]. If the parameter σ is larger, the smoothing ability of the function is stronger, the local minimum of the edge indicator function is small. The remnants of noise and texture are less in the smoothed image. But the edge is severely blurred when the Gaussian smoothing is employed with the larger parameter σ . It causes over-convergence in image segmentation. If the parameter σ is small, the remnants of noise and texture are more in the smoothed image, and the local minimum of the edge indicator function is large.

The basic idea of the sequential filter is by using small filtering parameter to replace the larger filtering parameter. This can effectively avoid severely smoothing of the edges. Assuming the image u is smoothed using the sequential Gaussian filter with the different parameter, respectively σ_1, σ_2 , the smoothed image \tilde{u} is:

$$\tilde{u} = u^* g(\sigma_1)^* g(\sigma_2) = u^*(g(\sigma_1)^* g(\sigma_2)) \quad (1)$$

Given:

$$\begin{aligned} g(\sigma_3) &= g(\sigma_1)^* g(\sigma_2) \\ &= \int_{-\infty}^{+\infty} e^{-\frac{x^2}{2\sigma_1^2} - \frac{(t-x)^2}{2\sigma_2^2}} dx \\ &= e^{-\frac{t^2}{2(\sigma_1^2 + \sigma_2^2)}} \int_{-\infty}^{+\infty} e^{-(\sigma_1^2 + \sigma_2^2) \left(x - \frac{\sigma_1^2}{\sigma_1^2 + \sigma_2^2} t\right)^2 / 2\sigma_1^2 \sigma_2^2} dx \\ &= \sqrt{2\pi} \sigma_1 \sigma_2 / \sqrt{(\sigma_1^2 + \sigma_2^2)} e^{-\frac{t^2}{2(\sigma_1^2 + \sigma_2^2)}} \end{aligned} \quad (2)$$

Observed the (2), the effect of smoothing which using the sequential filter with the parameter σ_1, σ_2 , is equal to that with the parameter σ_3 .

$$\sigma_3 = \sqrt{\sigma_1^2 + \sigma_2^2} \quad (3)$$

Especially, when $\sigma_1 = \sigma_2 = \sigma$, the parameter $\sigma_3 = \sqrt{2}\sigma$. The relationship between the filtering times and equivalent variance is shown in Fig.1.

B. THE RANDOM WALKS

Random walks algorithm is an interactive image segmentation that is based on graph theory. Image to be segmented was firstly converted to the weighted undirected graph. Then, according to the texture, luminance, and chroma information, the weight of the edge is designed. The weight describes how similar the nodes are. Grady uses Gaussian weighting function to describe the edge weights as given by:

$$w_{ij} = \exp[-\beta(h_i - h_j)^2] \quad (4)$$

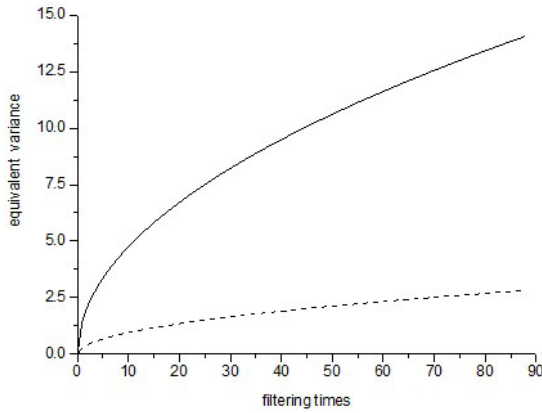


FIGURE 1. The relationship between the filtering times and equivalent variance . On solid curve $\sigma = 1.5$ and on dash dot curve $\sigma = 0.3$.

Where, w_{ij} is the edge weight, h_i and h_j are the intensity of pixel i and j , and β is the adjustable parameter as described in [17].

The probability matrix is introduced, for every free pixel i (unlabeled) , the matrix $P_{\text{foreground}}$ stores the probability of i reach the foreground seed. Similarly, $P_{\text{background}}$ is also. When there are only two kinds of seeds in experiments, the $P_{\text{foreground}}$ and $P_{\text{background}}$ have the following relationship:

$$P_{\text{foreground}} = 1 - P_{\text{background}} \quad (0 \leq P_{\text{foreground}}, P_{\text{background}} \leq 1) \quad (5)$$

As for pulmonary nodule segmentation, traditional random walks algorithm asks the users to manually mark the seeds (the foreground seeds and the background seeds). Then, according to the discrete theory, the pulmonary nodule could be segmented. This method is insensitive to noise and performs well on weak edge. It has satisfactory time consumption for small size images, but with the image pixels increasing, the time consumption becomes larger.

III. SEGMENTATION OF SOLITARY PULMONARY NODULE

To implement the SPN segmentation of DR, the proposed method needs to undergo following steps: Firstly, after simple preprocessing procedures, the original image is decomposed. By using the boundary estimation and the curve transformation, the set of seeds will be acquired. Then, our proposed selection tactic is employed to reduce the computational cost. Lastly, random walks algorithm which integrates sequential filter is used to segment the SPN.

A. FAST AND ADAPTIVE SEEDS SELECTION TACTIC

Random walks is a semi-supervised algorithm, and it needs the users to mark the seeds manually, which is not suitable for computer-aided diagnosis (CAD) system. To overcome this, scholars have done a lot of researches on automatic seeds selection. The [19] gives a solution which focus on mammograms mass. This method needs several rounds of iteration and estimation, it leads to logically complex and time-consuming algorithm. In this paper, we give a clear and time-saving solution.

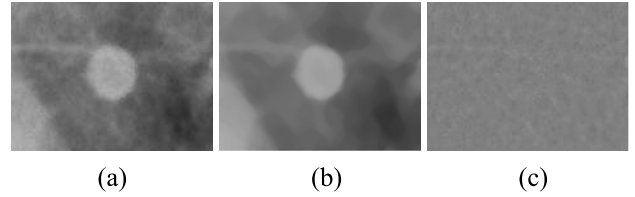


FIGURE 2. SPN image decompositions (a) original pulmonary nodule image (b) the cartoon component of (a) (c) the texture component of (a).

The imaging characteristic of the nodule is: the intensity is relatively high in center and decreases with the outward extension. The intensity changes slowly at the edge, and the segmentation is easily affected by the infiltrate tissue, texture and so on. More often, the nodules are embedded in the surrounding tissues, which makes it difficult to fix the position of edges. To get the effective seeds, inspired by Meyer’s texture retention model [21], original image $I(x, y)$ is decomposed into the cartoon and the texture components, as:

$$I(x, y) = u(x, y) + v(x, y) \quad (6)$$

Where $u(x, y)$ is the cartoon component, and $v(x, y)$ is the texture component. The cartoon component (as Fig.2.b shows) contains the main structure of the image and the slow variation parts. And the texture component (as Fig.2.c shows) includes small scale details and random noise.

The [22] proposed an effective edge method for the blurry images. This method can extract the thin edge and remove the false edge which is suitable for the SPN images. In this paper, to get the seeds, firstly, we use the edge detection method in [22] to achieve the quasi edge points, as shown in Fig.3.a. Then, the ellipse fitting method is employed to get an ellipse which is as close as possible to the quasi edge points, as shown in Fig.3.b. In this step, accurate nodule boundary is not a must. Finally, shrinking the above fitting curve by half, which guarantees the points of the deformed ellipse all locates in the lesions area. The points of the deformed curve are labeled as foreground seeds, as the yellow curve shown in Fig.3.c. The dilation operation of mathematical morphology is utilized on the fitted ellipse, a disk of 15 pixels is selected by experiment to make the new curve covers SPN, the green curve shown in Fig.3.c are the background seeds.

Hong [23] and Grady [17] found that the background seeds which surround the region of interest (ROI) can avoid the walkers outside the curve walking into it. Obviously, it guarantees the effective of the accuracy of segmentation. From the seeds labeling in Fig.3c, a large amount of seeds have been selected. There is no doubt that it brings computing cost. To solve this, firstly, we draw the inscribed circle of the foreground curve and the circumcircle of the background curve. Secondly, we divided the structure into several equal sections. In this paper, sixteen sections was selected to ensure the seeds relatively uniformly distributed. Finally, from each section, a certain number of foreground and background seeds were

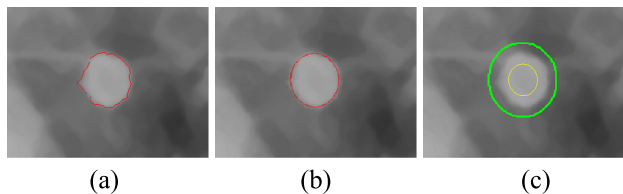


FIGURE 3. Get the foreground and background seeds (a) Boundary estimate (b) Ellipse fitting (c) foreground seeds (yellow curve) and background seeds (green curve).

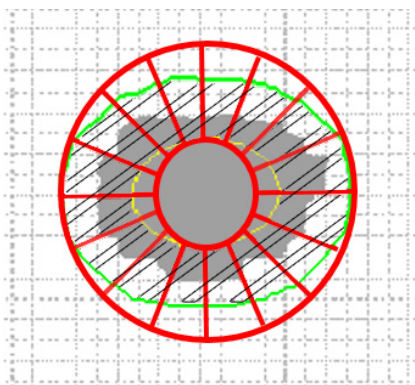


FIGURE 4. The sketch map of the seeds and walker pixels selection tactic.

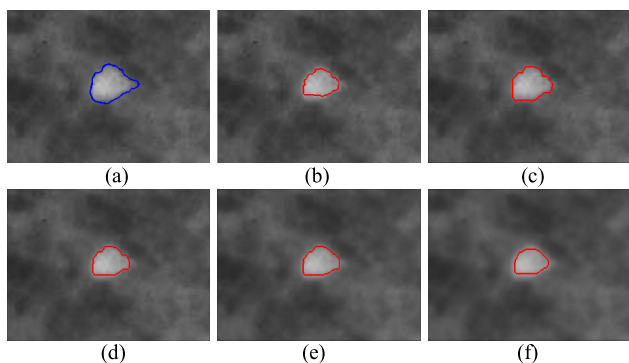


FIGURE 5. The effect of filtering times on segmentation results (a)the ground truth (b)-(f) 5,15,30,40,60 times filtering, respectively.

randomly selected. In this paper, we set the number of seeds as four by experiment. For better understanding, the sketch map is shown as Fig.4. The gray area represents the SPN, the green and yellow curve are the curve of background and foreground seeds, respectively. Two red circles are inscribed and circumscribed circle. In addition, the pixels outside the background curve (green curve) and inside the foreground curve (yellow curve) could be marked as background and the pulmonary nodule, respectively. Only the pixels in area with slant lines (seen Fig.4.) will be taken into the computation, which makes the walking algorithm speed up.

B. IMPROVED ADAPTIVE RANDOM WALKS SEGMENTATION WITH SEQUENTIAL FILTER

In our previous work [24], the sequential filter was introduced into active contour models. It performs well on natural images, but badly on DR pulmonary nodule, especially on nodules with obscure edge. Unlike active contour models, random walks algorithm has advantage on medical images.

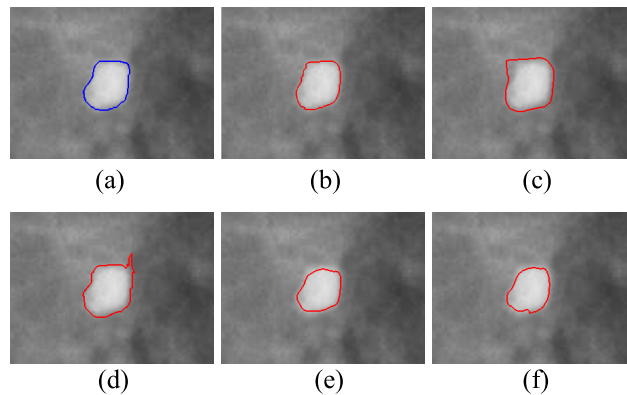


FIGURE 6. Comparison of the segmentation method on homogenous image with clear margin (a) the ground truth (b) the proposed method (c) CV (d) IMST (e) SFAC (f) ITV.

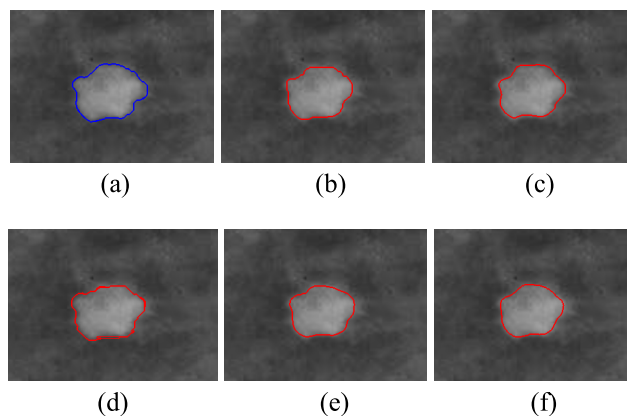


FIGURE 7. Comparison of the segmentation method on homogenous image with obscured margin (a) the ground truth (b) the proposed method (c) CV (d) IMST (e) SFAC (f) ITV.

It can handle the smoothly varying characteristics of the edge, even the partial edge deletion. The [17] provides the demonstration response to the partial edge deletion. And the [19] shows the application on mass segmentation of mammogram in which there exist smoothly varying edges.

As in equation (3), the effect of the sequential filter with small variance and that of the Gauss filter with large variance are almost identical. This inspires us, the random walk which incorporates sequential filter can suppress the effect of surrounding structure and avoid over-smoothing. Traditional random walking runs just one round which is easily affected by the uncertainty factors, such as redundant texture, noise, ill-defined tissues. Sequential filter could handle the texture and noise, avoid over-smoothing, but needs several rounds running. To cope with this, we incorporate the sequential filter theory into the adaptive random walking model, and construct a novel model for DR SPN segmentation, as defined by:

$$\begin{cases} I_n = I_{n-1} * g(\sigma) \\ w_{ij} = \exp(-\beta (h_i^n - h_j^n)^2) \\ P_F = \frac{1}{n} \sum_{t=1}^n P_{foreground}^t, \quad P_B = 1 - P_F \end{cases} \quad (7)$$

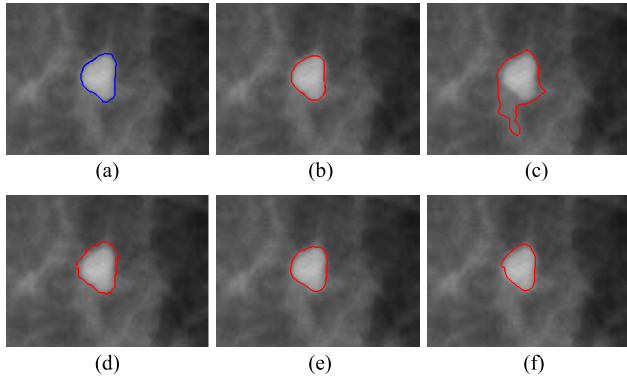


FIGURE 8. Comparison of the segmentation method on image with texture (a) the ground truth (b) the proposed method (c) CV (d) IMST (e) SFAC (f) ITV.

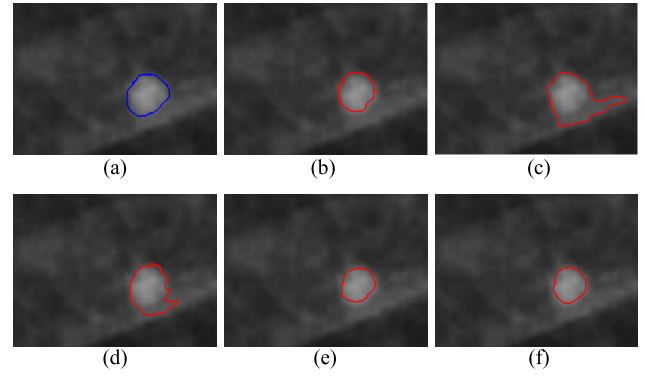


FIGURE 9. Comparison of the segmentation method on blurred image (a) the ground truth (b) the proposed method (c) CV (d) IMST (e) SFAC (f) ITV.

Where I_n is the image after the n th filtering, and h_i^n is the intensity of pixel i after the n th filtering. P_F and P_B are the proposed method's probability matrices, $P_{foreground}^t$ is the foreground probability matrix of the t^{th} filtering.

The proposed segmentation is described as follows:

program Image Segmentation (Output)

{Initial: k and $I_0 = I$ }

n is the number of the sequential filter and random walking
 k is the terminal condition of n

Begin

Decomposing the original ROI I_n into cartoon component $u(x, y)$ and texture component $v(x, y)$;

Estimating the boundary on the cartoon component $u(x, y)$;

Ellipse fitting based on the previous step, shrinking and dilating the fitting ellipse.

Section based seeds selection tactic

$n := 0$;

Repeat

Sequential filtering applied to I_n ;

Adaptive seeds selection Random Walking on the result of the previous step, computing newly defined edge weights w_{ij} , probability matrixs P_F and P_B uses:

$$w_{ij} = \exp[-\beta(h_i - h_j)^2] \quad (8)$$

and

$$P_F = \frac{1}{n} \sum_{t=1}^n P_{foreground}^t \quad // \text{definition see formula (7)}$$

$$P_B = 1 - P_F$$

Until

$n \geq k$ //The terminal condition:

Output: the result of segmentation.

End

IV. EXPERIMENTAL RESULTS

The experiments are conducted using MATLAB on the PC with Intel-Core i5 CPU 3.20GHz and 2GB of RAM without any particular code optimization. The DR pulmonary nodule images shown in this paper are from the Japanese

Society of Radiological Technology database (JSRT) and the ‘‘National Twelfth Five-Year Plan’’ Sichuan Province Major Infectious Disease Special Demonstration Project-Tuberculosis database. These two databases are covering extensively, includes lung cancer, pulmonary nodule, emphysema and so on. In our study, we collected 724 cases of SPN from a total of 2664 lung DR images.

A. EVALUATION METRICS

Common evaluation metrics such as precision, recall and F-measure are universally agreed on, standard, and easy-to-understand measures for evaluating a segmentation model. The precision focus on the proportion of the real target area in the segmentation results. The recall focus on the proportion of the proper segmentation region in the region of concern. Precision and recall reflect the relationships between ground truth and segmentation regions. However, precision and recall indicators sometimes show contradictory situation. So the F-measure is proposed as a weighted harmonic average of them.

$$\begin{cases} \text{precision} = |Mask \cap GT|/|Mask| \\ \text{recall} = |Mask \cap GT|/|GT| \\ \text{F-measure} = 2 \times \text{precision} \times \text{recall}/(\text{precision} + \text{recall}) \end{cases} \quad (9)$$

Where $Mask$ is the binary mask which covers the segmentation region of the object, and GT is the ground-truth.

B. DISCUSSION

In the algorithm description (at the end of section III B), we give a parameter k which is the terminal condition of parameter n . In our proposed model, the image is smoothed using sequential filter, and smoothing performance depends on the number of filtering. To analyze the relationship between filtering times n and segmentation performance, a 300*224-pixel SPN image with infiltrated boundary and fog-like texture is smoothed with different times of filtering, and partial results of segmentation are shown in Fig.5. . When n is small, the SPN region is inhomogeneous, the intensity of

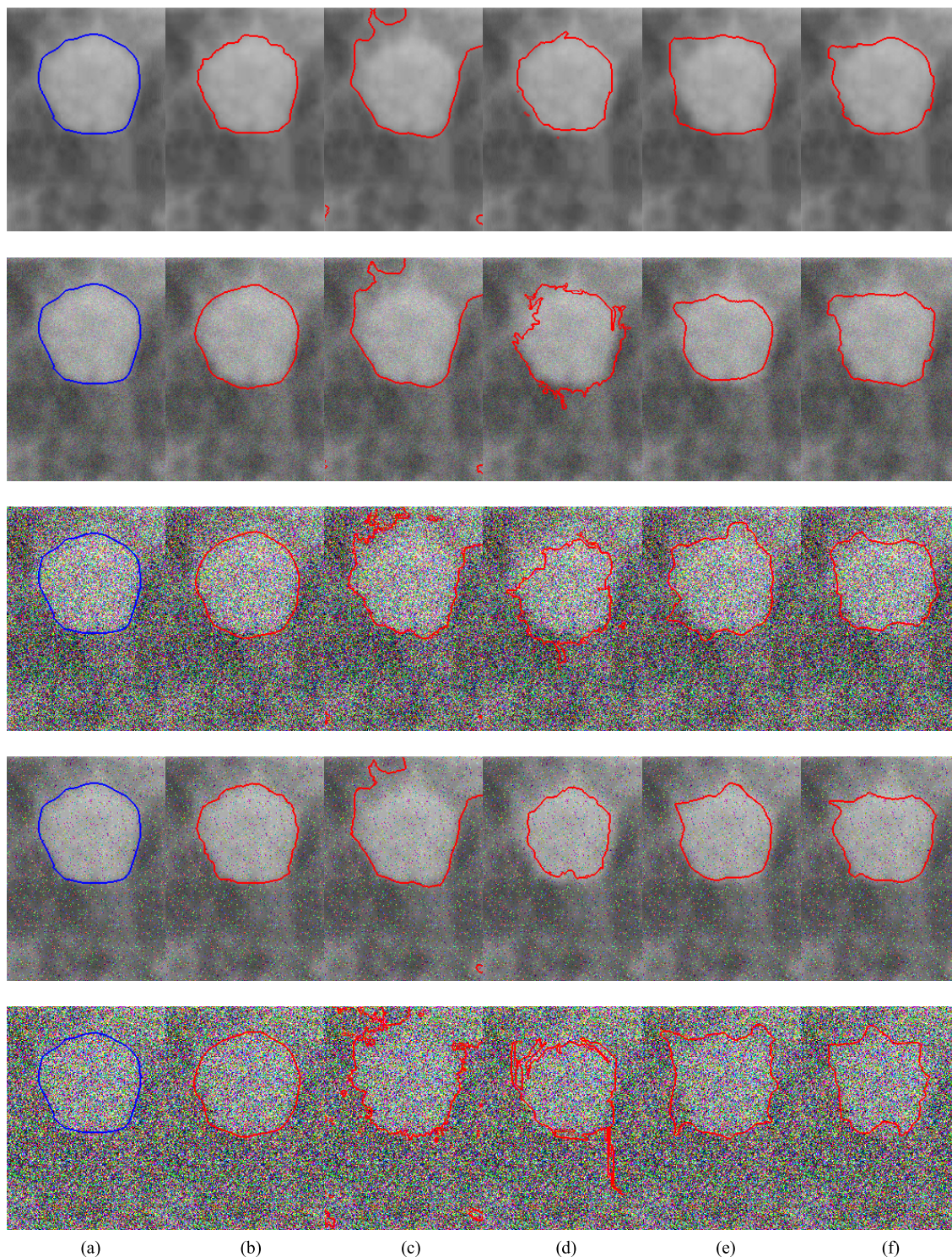


FIGURE 10. Comparison of the segmentation methods on image with noise (a) the ground truth (b) the proposed method (c) CV (d) IMST (e) SFAC (f) ITV. Row 1: the original image; row 2-3: image with Gaussian noise, the PSNR are 37.9406 and 31.4725, respectively; row 4-5: image with salt-and-pepper noise, the PSNR are 35.9302 and 30.8374, respectively;

the center region is higher than the boundaries, and the texture around SPN structure is clear. The first arrival probabilities which from pixels around the boundaries to background seeds are higher. This leads to the poor results, as shown in Fig.5.b.

When n is large, the edge of the SPN is severely blurred which will cause the over-segmentation results, as Fig.5.f shows. The evaluation metrics of segmentation with different parameters n are listed in Table I. From Table I, the precisions are

TABLE 1. Evaluation metrics of image segmentation with filtering number (n).

metric \ N	N						
	5	10	15	20	30	40	60
precision	1.000	1.000	0.999	0.998	0.999	0.999	1.000
recall	0.566	0.573	0.818	0.800	0.792	0.782	0.548
F-measure	0.723	0.729	0.900	0.888	0.883	0.877	0.708

TABLE 2. CPU time and score of segmentation comparison of Fig.6.-Fig.9.

image and size method and metrics	Fig.6	Fig.7	Fig.8	Fig.9
	300×224	508×380	380×280	480×360
The proposed method				
precision	0.936	1.000	0.966	0.916
recall	0.990	0.865	0.924	0.796
F-measure	0.962	0.928	0.945	0.852
CPU time (s)	7.511	18.425	8.212	15.190
CV model				
precision	0.732	0.996	0.572	0.613
recall	1.000	0.844	0.998	0.957
F-measure	0.846	0.914	0.727	0.748
CPU time (s)	1.330	6.398	2.010	5.624
IMST model				
precision	0.776	0.984	0.843	0.786
recall	1.000	0.897	0.988	0.884
F-measure	0.874	0.939	0.910	0.832
CPU time (s)	2.221	5.420	2.782	3.186
SFAC model				
precision	0.987	0.999	0.958	1.000
recall	0.777	0.813	0.934	0.638
F-measure	0.870	0.897	0.946	0.779
CPU time (s)	1.112	5.640	1.460	4.330
ITV model				
precision	1.000	1.000	0.955	1.000
recall	0.803	0.788	0.839	0.647
F-measure	0.891	0.881	0.893	0.786
CPU time (s)	12.037	30.886	12.073	26.757

almost identical. When $n = 15$, the recall and F-measure are higher, as the bold numbers in Table I; and the segmentation result is the closest to the ground truth, as Fig.5.c. In order to get better segmentation results, we suggest to choose $n = 15$ as the terminal condition of parameter n .

C. SEGMENTATION ALGORITHMS COMPARISON

To test the segmentation performance using the proposed method on SPN images, in this section, the experiments are carried on to compare with other four methods as below. The choice of these algorithms is motivated by the following reasons: Janakiraman [25] proposed a segmentation algorithm that used the improved minimum spanning tree (abbreviated as IMST). IMST and the proposed method are both based on graph theory. Our previous work [24] is an algorithm of active contour segmentation method, and it also employs the sequential filter (abbreviated as SFAC). He's model [26] employs the improved total variation algorithm (abbreviated as ITV), which could smooth the inhomogeneous sub-regions and preserve edge. It performs well on objects with

obscure edges. Beside these three new algorithms, we also choose a traditional and effective segmentation algorithm, Chan and Vese [15] active contour model (abbreviated as CV). The effects of the five algorithms on the homogenous SPN image are shown in Fig.6-7. In Fig.6, background and object region are homogenous, the SPN shows a relative clear margin, but the intensity difference between the object and the background is not significant. The CV and IMST method are under-segmentation, the evolution curve of the CV doesn't converge to the object boundary, IMST views partial background as the target region and adds the wrong pixels into the spanning tree (see Fig.6.c-d). The results of other models are similar, but the proposed method is better (see Fig.6.b,e,f). The mean of F-measures and the F-measure of the proposed method are 0.752 and 0.930, respectively. The CPU time of the proposed method in Fig.6. (300*224-pixel) and Fig.7. (480*320-pixel) are 9.672 and 30.84, as shown in Table II.

The texture is a key factor to that will affect the segmentation performance. To test if this algorithm could handle texture, the result of segmentation using a 320×221 -pixel image is shown in Fig.8.. At the lower left part of the lesion, there exists weak edges. The back ground is full of texture and the intensity is inhomogeneous. The locations of contour with CV model are far away from the true boundaries. The evolution curve of ITV converge to the inner of SPN. The mean of F-measures, the F-measure of the proposed method and IMST are 0.752, 0.945 and 0.898, respectively.

Moreover, poor image definition is one of the problems to be faced in DR image processing. Fig.9. is a blurred image where the SPN is affected by rib. Segmentation result of the IMST is poor, even worse in CV. Due to the vague margin, SFAC and ITV have varying degrees of over-segmentation. The proposed method is closer to the ground truth than others. The mean of F-measure and the F-measure of the proposed method are 0.710, 0.942, respectively.

Compared to the other four models, most of the segmentation accuracy of the proposed method is better and closer to the ground truth. By looking at smoothing number, CV model does not smooth, whilst IMST model only needs one time of Gaussian smoothing. The proposed method, SFAC and ITV models use iteration smoothing to achieve better result. Therefore, these three methods are time-consuming. Both the proposed method and the IMST model are based on graph theory, the size of image also affects the CPU-time. Table II shows the difference of CPU-time with different segmentation models.

To test if the proposed method is insensitive to noise, two common kinds of noise, the Gaussian noise and salt-and-pepper noise, were employed. The experiments on the degraded image are conducted and compared with CV, IMST, SFAC and the ITV models, as shown in Fig.10.. With the decreasing of the PSNR, IMST wrongly added some noise pixels into the minimum spanning tree, which causes the results contain the prominent structure, especially when the PSNR is lower, as the 3rd and 5th row in Fig.10..

TABLE 3. Scores of segmentation models on noisy images (the Pre and F-M denote precision and F-measure, G and SP denote Gaussian noise and salt-and-pepper noise, respectively. N is the name of noise).

Model and metric PSNR-N	The proposed method		CV model		IMST model		SFAC model		ITV model	
	Pre	F-M	Pre	F-M	Pre	Pre	F-M	Pre	F-M	Pre
37.9406-G	0.936	0.960	0.648	0.783	0.854	0.886	0.992	0.876	0.914	0.940
36.4712-G	0.889	0.955	0.652	0.783	1.000	0.890	0.768	0.869	0.971	0.950
31.4725-G	0.927	0.932	0.654	0.786	0.852	0.842	0.867	0.913	0.892	0.919
31.1465-G	0.845	0.916	0.651	0.782	1.000	0.808	0.660	0.795	0.869	0.912
40.8618-SP	0.989	0.972	0.646	0.787	0.936	0.913	0.877	0.93	0.944	0.961
35.9302-SP	0.983	0.964	0.648	0.783	1.000	0.86	0.997	0.912	0.967	0.949
33.461-SP	0.927	0.955	0.643	0.778	0.864	0.885	0.820	0.889	0.895	0.937
30.8374-SP	0.912	0.953	0.631	0.770	0.894	0.842	0.817	0.886	0.883	0.896
Original image	0.991	0.974	0.646	0.784	0.994	0.937	0.885	0.933	0.935	0.953
Mean	0.933	0.953	0.647	0.782	0.933	0.874	0.854	0.89	0.919	0.935
Standard Deviation	0.046	0.018	0.006	0.005	0.063	0.037	0.099	0.04	0.035	0.02

TABLE 4. The score of the evaluation metrics based on The data set (the Pre, Rec and F-M denote precision, recall and F-measure, respectively).

Metric Method	Mean			Standard Deviation		
	Pre	Rec	F-M	Pre	Rec	F-M
The proposed method	0.954	0.895	0.922	0.028	0.072	0.038
CV model	0.725	0.931	0.802	0.148	0.068	0.069
IMST model	0.844	0.93	0.882	0.074	0.052	0.038
SFAC model	0.986	0.803	0.881	0.015	0.098	0.057
ITV model	0.983	0.847	0.898	0.02	0.066	0.042

SFAC with the variable Gauss kernel function is better than the CV model, however, the noise blurs the edge of the ROI, the level set curve cannot locate accurately. ITV employs the improved anisotropic smoothing and total variation method to keep relatively stable results. Nevertheless, when the PSNR is low, the nodule in object regions was separated. In the proposed method, the background seeds prevent the walkers from walking outside, which guarantees positional accuracy, and the sequential filtering removes the noise of images. The scores of different models with different PSNR and noise are shown in Table III.

From Table III, the precision and the F-measure of these five models keep the downward tendency with the PSNR decreasing. The mean of F-measure in the proposed method, CV model, the IMST model, the SFAC model and the ITV model are 0.953, 0.782, 0.874, 0.89 and 0.935, respectively. Higher mean of evaluation metrics give better results, and lower standard deviation means more stable performance. The mean of F-measure in the proposed method is the highest compared to others. Meanwhile, the standard deviation of the F-measure are 0.018, 0.005, 0.037 and 0.02, respectively. The standard deviations of CV and the proposed method are lower, however, the mean of the CV model is just 0.782. The proposed method performs better than other four methods on noisy images.

The experimental data set in our study consists of 724 cases of SPN. Based on this data set, we give the statistical results on precision, recall, F-measure, mean and standard deviation, as shown in Table IV. The mean of the F-measure in the

proposed method is higher, that is 0.922 as shown in bold. It means that the proposed method gets better results than others. The lower standard deviation the methods gets, the more stable performance the methods achieve. The standard deviation of the F-measure in the proposed method and IMST are almost the same, those are both 0.038. However, the mean of F-measure in IMST is 0.882. From the statistics of our comparison analysis, our proposed method have attained a better and relatively stable segmentation result.

V. CONCLUDING REMARKS

In order to achieve an automatic segmentation of SPN in DR images, a new image segmentation model is proposed. By comparison analysis above, the proposed method have attained more accurate results and dealt inhomogeneous sub-regions. However, the CPU-time of the proposed method is higher, which caused by the times of smoothing and walking. So, in our further study, we plan to optimize parameters of smoothing and discuss the relationship between filtering and walking techniques. Moreover, split Bergman method is effective method which could be introduced to improve the performance of the sequential filtering in the future.

REFERENCES

- [1] J. K. Field, A. Devaraj, S. W. Duffy, and D. R. Baldwin, "CT screening for lung cancer: Is the evidence strong enough?" *Lung Cancer*, vol. 91, pp. 29–35, Jan. 2016.
- [2] G. Rossi, A. Cavazza, C. Casali, A. M. Cesinaro, F. Cinquantini, and U. Morandi, "Tuberous sclerosis complex presenting as a pulmonary solitary nodule," *Histopathology*, vol. 48, no. 6, pp. 769–771, 2006.
- [3] K. Nakagomi, A. Shimizu, H. Kobatake, M. Yakami, K. Fujimoto, and K. Togashi, "Multi-shape graph cuts with neighbor prior constraints and its application to lung segmentation from a chest CT volume," *Med. Image Anal.*, vol. 17, no. 1, pp. 62–77, 2013.
- [4] R. M. Harrison, "Digital radiography," *Phys. Med. Biol.*, vol. 33, no. 7, pp. 751–784, 1988.
- [5] A. C. Kak and M. Slaney, "Principles of computerized tomographic imaging," *Med. Phys.*, vol. 29, no. 1, p. 107, 2002.
- [6] H. Hatabu, Q. Chen, K. W. Stock, W. B. Gefter, and H. Itoh, "Fast magnetic resonance imaging of the lung," *Eur. J. Radiol.*, vol. 29, no. 2, pp. 114–132, 1999.
- [7] T. A. Bley et al., "Comparison of radiologist and CAD performance in the detection of CT-confirmed subtle pulmonary nodules on digital chest radiographs," *Invest. Radiol.*, vol. 43, no. 6, pp. 343–348, 2008.

- [8] S. G. Armato, III, et al., "Lung image database consortium: Developing a resource for the medical imaging research community," *Radiology*, vol. 232, no. 3, pp. 739–748, 2004.
- [9] X. Lu, X. Wang, D. Li, X. Wang, and J. Wu, "Comparative study of DR and CT in the application of close contacts screening for tuberculosis outbreaks," *Radiol. Infectious Diseases*, vol. 3, no. 1, pp. 34–39, 2016.
- [10] J. E. Takasugi and J. D. Godwin, "The solitary pulmonary nodule: Radiologic assessment," in *Radiologic Diagnosis of Chest Disease*. London, U.K.: Springer, 2001, pp. 462–484.
- [11] S. Mitra and B. Barman, "Rough-fuzzy clustering: An application to medical imagery," in *Proc. Int. Conf. Rough Sets Knowl. Technol.*, 2008, pp. 300–307.
- [12] C. Bahlmann, X. Li, and K. Okada, "Local pulmonary structure classification for computer-aided nodule detection," *Proc. SPIE*, pp. 61445I-1–61445I-11, 2006.
- [13] S. Y. Yuen and C. H. Ma, "Genetic algorithm with competitive image labelling and least square," *Pattern Recognit.*, vol. 33, no. 12, pp. 1949–1966, 2000.
- [14] V. Raman, P. Sumari, and P. Then, "MATLAB implementation and results of region growing segmentation using haralick texture features on mammogram mass segmentation," in *Advances in Wireless, Mobile Networks and Applications*. Berlin, Germany: Springer, 2011, pp. 293–303.
- [15] S. Kichenassamy, A. Kumar, P. Olver, A. Tannenbaum, and A. Yezzi, "Gradient flows and geometric active contour models," in *Proc. IEEE Comput. Soc. Int. Conf. Comput. Vis.*, Jun. 1995, pp. 810–815.
- [16] T. F. Chan and L. A. Vese, "Active contours without edges," *IEEE Trans. Image Process.*, vol. 10, no. 2, pp. 266–277, Feb. 2001.
- [17] L. Grady, "Random walks for image segmentation," *IEEE Trans. Pattern Anal. Mach. Intell.*, vol. 28, no. 11, pp. 1768–1783, Nov. 2006.
- [18] C. Qin, G. Zhang, G. Li, L. Chen, and J. Ge, "Multiclass color-texture image segmentation based on random walks framework integrating compact texture information," in *Proc. 3rd Int. Conf. Multimedia Technol. (ICMT)*, 2014, pp. 357–364.
- [19] X. Hao, Y. Shen, and S.-R. Xia, "Automatic mass segmentation on mammograms combining random walks and active contour," *J. Zhejiang Univ. SCI. C*, vol. 13, no. 9, pp. 635–648, 2012.
- [20] A. Goshtasby and M. Satter, "An adaptive window mechanism for image smoothing," *Comput. Vis. Image Understand.*, vol. 111, no. 2, pp. 155–169, 2008.
- [21] Y. Meyer, *Oscillating Patterns in Image Processing and Nonlinear Evolution Equations: The Fifteenth Dean Jacqueline B. Lewis Memorial Lectures*, vol. 22. American Mathematical Society, 2001, p. 122.
- [22] J. Wu, Z. Yin, and Y. Xiong, "The fast multilevel fuzzy edge detection of blurry images," *IEEE Signal Process. Lett.*, vol. 14, no. 5, pp. 344–347, May 2007.
- [23] B.-W. Hong and B.-S. Sohn, "Segmentation of regions of interest in mammograms in a topographic approach," *IEEE Trans. Inf. Technol. Biomed.*, vol. 14, no. 1, pp. 129–139, Jan. 2010.
- [24] D. Wang, K. He, and X. Zhang, "The level set image segmentation on sequential filtering," *J. Sichuan Univ.*, vol. 53, no. 3, pp. 518–525, 2016. [Online]. Available: http://science.ijournals.cn/jsunature_cn/ch/reader/view_abstract.aspx?file_no=W150334&flag=1
- [25] T. N. Janakiraman and P. V. S. S. R. Chandra Mouli, "Image segmentation based on minimal spanning tree and cycles," in *Proc. Int. Conf. Comput. Intell. Multimedia Appl.*, vol. 3, Dec. 2007, pp. 215–219.
- [26] K. He, D. Wang, and X. Zhang, "Image segmentation using the level set and improved-variation smoothing," *Comput. Vis. Image Understand.*, vol. 152, pp. 29–40, Nov. 2016.



DAN WANG received the bachelor's degree in software engineering from Sichuan University in 2014. She is currently a Graduate Student of the Software Engineer, the Key National Defense Laboratory of Visual Synthesis Graphic and Image, Sichuan University. Her major work was pattern recognition, image processing, and medical image analysis.



JUNFENG WANG received the Ph.D. degree in computer science from the University of Electronic Science and Technology of China, Chengdu, in 2004. From 2004 to 2006, he held a post-doctoral position at the Institute of Software, Chinese Academy of Sciences. Since 2006, he has been a Professor with the College of Computer Science, Sichuan University. His research interests include spatial information networks, network and information security, intelligent transportation system, and medical image processing.



YIHUA DU was an Expert with the Ministry of Health of China Aid Mozambique Medical Team, from 1994 to 1996. He is currently the Director of the Affiliated Hospital of Southwest Medical University, China. He is the Expert of General Surgery and Tumor. He has published more than ten academic papers in the medical area.



PENG TANG received the bachelor's degree in automation from Chongqing University, Chongqing, China, in 2002, and the Ph.D. degree in computer application and technology with an emphasis on imaging and vision from Sichuan University, Chengdu, China, in 2010. He is currently a Lecturer with Southwest Jiaotong University, China. His research interests include the area of computer vision and machine learning, with contributions in robotic vision, medical image processing, and video understanding.

• • •